Development/Plasticity/Repair

Cell-Autonomous Inactivation of the Reelin Pathway Impairs Adult Neurogenesis in the Hippocampus

Catia M. Teixeira,[1]* Michelle M. Kron,[2]* Nuria Masachs,[1]* Helen Zhang,[2] Diane C. Lagace,[4] Albert Martinez,[1] Isabel Reillo,[8] Xin Duan,[5] Carles Bosch,[1] Lluis Pujadas,[1] Lucas Brunso,[1] Hongjun Song,[5] Amelia J. Eisch,[6] Victor Borrell,[8] Brian W. Howell,[7] Jack M. Parent,[2,3] and Eduardo Soriano[1]****

[1]Developmental Neurobiology and Regeneration Laboratory, IRB Barcelona, Parc Cientific de Barcelona, Centro de Investigación Biomédica en Red sobre Enfermedades Neurodegenerativas (CIBERNED, ISCIII), Department of Cell Biology, University of Barcelona, Barcelona E-08028, Spain, [2]Department of Neurology and Neuroscience Graduate Program, University of Michigan Medical School, Ann Arbor, Michigan 48109, [3]Ann Arbor Veterans Administration Healthcare System, Ann Arbor, Michigan 48105, [4]Department of Cellular and Molecular Medicine, University of Ottawa, Ottawa, Ontario K1H 8M5, Canada, [5]Institute for Cell Engineering, Departments of Neurology and Neuroscience, Johns Hopkins University School of Medicine, Baltimore, Maryland 21205, [6]Department of Psychiatry, University of Texas Southwestern Medical Center, Dallas, Texas 75390-9070, [7]Department of Neuroscience and Physiology, State University of New York, Syracuse, New York 13210, and [8]Instituto de Neurociencias, Consejo Superior de Investigaciones Científicas-Universidad Miguel Hernández, Sant Joan d'Alacant E-03550, Spain

Adult hippocampal neurogenesis is thought to be essential for learning and memory, and has been implicated in the pathogenesis of several disorders. Although recent studies have identified key factors regulating neuroprogenitor proliferation in the adult hippocampus, the mechanisms that control the migration and integration of adult-born neurons into circuits are largely unknown. Reelin is an extracellular matrix protein that is vital for neuronal development. Activation of the Reelin cascade leads to phosphorylation of Disabled-1, an adaptor protein required for Reelin signaling. Here we used transgenic mouse and retroviral reporters along with Reelin signaling gain-of-function and loss-of-function studies to show that the Reelin pathway regulates migration and dendritic development of adult-generated hippocampal neurons. Whereas overexpression of Reelin accelerated dendritic maturation, inactivation of the Reelin signaling pathway specifically in adult neuroprogenitor cells resulted in aberrant migration, decreased dendrite development, formation of ectopic dendrites in the hilus, and the establishment of aberrant circuits. Our findings support a cell-autonomous and critical role for the Reelin pathway in regulating dendritic development and the integration of adult-generated granule cells and point to this pathway as a key regulator of adult neurogenesis. Moreover, our data reveal a novel role of the Reelin cascade in adult brain function with potential implications for the pathogenesis of several neurological and psychiatric disorders.

Introduction

Neurogenesis persists throughout adulthood in the hippocampal dentate gyrus (DG) (Altman and Das, 1965; Cameron et al., 1993; Kuhn et al., 1996). Continuous generation of neurons in the adult hippocampus is essential for learning and has been proposed recently to contribute to the development of psychiatric disorders (Eisch et al., 2008). DG neuroblasts arise in the subgranular zone, migrate a short distance into the granule cell layer (GCL), and differentiate into dentate granule cells (DGCs) (van Praag et al., 2002; Ge et al., 2008; Toni et al., 2008). Thus, adult neurogenesis is a multistep process comprising the regulation of stem cell niches, cell proliferation, differentiation and *de novo* formation of dendrites and axons, and the integration of adult-generated neurons into functional circuits. While recent studies have identified key factors for the regulation and proliferation rates of neuroprogenitor cells, much less is known about the mechanisms that control the migration and functional recruitment of adult-generated neurons. *Disrupted in Schizophrenia-1* (*DISC1*), a schizophrenia susceptibility gene, was recently found to regulate process development and migration of adult-generated DGCs (Duan et al., 2007; Faulkner et al., 2008; Kim et al., 2009). Other molecules, including cyclin-dependent kinase 5 (cdk5), NeuroD, Sonic hedgehog, Prox1 and Wnts, are also implicated in controlling several steps of adult DGC neurogenesis (Lie et al., 2005; Jessberger et al., 2008; Lagace et al., 2008; Gao et al., 2009; Karalay

Received April 17, 2012; revised July 1, 2012; accepted July 9, 2012.

Author contributions: C.M.T., M.M.K., D.C.L., X.D., H.S., A.J.E., V.B., B.W.H., J.M.P., and E.S. designed research; C.M.T., M.M.K., N.M., D.C.L., H.Z., A.M., I.R., X.D., C.B., L.P., and L.B. performed research; D.C.L., X.D., H.S., A.J.E., V.B., and B.W.H. contributed unpublished reagents/analytic tools; C.M.T., M.M.K., N.M., H.Z., D.C.L., A.M., H.S., A.J.E., J.M.P., and E.S. analyzed data; C.M.T., M.M.K., D.C.L., H.S., A.J.E., B.W.H., J.M.P., and E.S. wrote the paper.

This project was supported by Grant BFU2008-3980 from the Ministerio de Ciencia e Innovacion (MICINN), Spain; by grants from the Centro de Investigación Biomédica en Red sobre Enfermedades Neurodegenerativas (CIBERNED) and Caixa Catalunya-Obra Social Foundations to E.S.; by grants from the Spanish Ministry of Science and Innovation (SAF2009-07367 and CONSOLIDER CSD2007-00023) to V.B.; by the Fred Annegers Fellowship from the Epilepsy Foundation (M.M.K.); and by NIH Grant NS058585 to J.M.P. I.R. was recipient of a Formación de Personal Universitario predoctoral fellowship from MINECO (Spain). We also thank Ashraf Muhaisen for technical help; Tanya Yates for editorial assistance; and F. Gage and S. Jessberger for reagents.

*C.M.T., M.M.K., and N.M. contributed equally to this study.

**J.M.P. and E.S. are co-senior authors.

Correspondence should be addressed to either of the following: Dr. Eduardo Soriano, IRB Barcelona, Baldiri Reixac 10, Barcelona E-08028, Spain, E-mail: eduardo.soriano@irbbarcelona.org; or Dr. Jack M. Parent, 5021 Biomedical Sciences Research Building, 09 Zina Pitcher Place, Ann Arbor, MI 48109. E-mail: parent@umich.edu.

DOI:10.1523/JNEUROSCI.1857-12.2012

 0270-6474/12/3212051-15$15.00/0

et al., 2011). Interestingly, spatial learning training accelerates the integration of adult-generated neurons, and dendritic spine formation in adult-born GCs is impaired in mouse (Ms) models of Alzheimer's disease (AD) (Sun et al., 2009; Lemaire et al., 2012).

Reelin is an extracellular matrix protein essential for neuronal migration during the development of laminated brain regions (D'Arcangelo et al., 1995; Tissir and Goffinet, 2003). This extracellular protein also regulates dendrite development, the formation of dendritic spines, and glutamatergic neurotransmission and neural plasticity (Chen et al., 2005; Herz and Chen, 2006; Qiu et al., 2006; Groc et al., 2007; Pujadas et al., 2010). A critical player in the Reelin pathway, Disabled-1 (Dab1), is an intracellular adaptor protein activated by Reelin binding to its receptors, apolipoprotein E receptor 2 (ApoER2) and very-low-density lipoprotein receptor (VLDLR) (Howell et al., 1997; Rice et al., 1998; D'Arcangelo et al., 1999; Hiesberger et al., 1999). Reelin expression persists into adulthood in hippocampal and cortical interneurons (Alcántara et al., 1998; Pesold et al., 1998).

Recent studies suggest that changes in Reelin expression contribute to the pathogenesis of several neurological diseases, including epilepsy, AD, and schizophrenia, all of which display abnormalities in GC neurogenesis and organization (Haas et al., 2002; Heinrich et al., 2006; Gong et al., 2007; Haas and Frotscher, 2010). Here we examined the involvement of the Reelin signaling pathway specifically in adult hippocampal neurogenesis. We show that this cascade dramatically regulates DG adult neurogenesis in a cell-autonomous manner. Whereas overexpression of Reelin accelerates dendritic maturation, disruption of the Reelin pathway results in aberrant dendritic development and orientation and in the formation of aberrant synaptic circuits.

Materials and Methods

Animals

Experiments were conducted in parallel in two independent laboratories, one at the Institute for Research in Biomedicine (IRB Barcelona) and the other at the University of Michigan. All animal procedures were performed in accordance with protocols approved by local ethics committees. Male Sprague Dawley rats were purchased from Charles River. For mouse experiments, a *NestinCreER^{T2}* line was crossed with a floxed-stop Rosa26-yellow fluorescent protein (*R26RYFP*) reporter line, both on a C57BL/6J background (Lagace et al., 2007). Either bigenic mice or *NestinCreER^{T2}* single-transgenic mice were then crossed with a Dab1-conditional knock-in line containing floxed dab1 alleles (*Dab1$^{flox/flox}$*) on a C57BL/6 background (Pramatarova et al., 2008). All animals were kept under a constant 12 h light/dark cycle and had access to food and water *ad libitum*.

Generation of plasmid DNA constructs

Vectors were made for overexpression or shRNA-mediated knockdown of Dab1. To generate the Dab1 overexpression vector [pDab1-IRES-mCherry (mCh)-woodchuck hepatitis virus posttranscriptional response element (WPRE)], a rat Dab1 cDNA was cloned into a retrovirus (RV) vector under the control of the CAG promoter. IRES, mCh, and WPRE were subcloned downstream of Dab1, and proper orientation was verified by sequencing. For shRNA vectors, constructs were generated with GFP (pUEG) expression under the control of the EF1α promoter and a specific shRNA (to Dab1 or to DsRed as a control) placed under the control of the human U6 promoter in the same vector (Duan et al., 2007). The Dab1 shRNA vector pSiE-U6-shDab1-EF1α-GFP contained a previously characterized shRNA against rodent Dab1 (Olson et al., 2006), and a control shRNA against DsRed (pSiE-U6-shDsRed-EF1α-GFP) was used as described previously (Ge et al., 2006). Short hairpin sequences were AATTTCTGAACCACGTCAGGGTT for Dab1 and AGTTCCAGTACGGCTCCAA for DsRed.

In vitro *studies*

293T cells were cultured onto four-well chamber slides in DMEM with 10% FBS for 20 h at 37°C. Two sets of experiments were performed. In the first, cells were transfected with plasmid DNA constructs pSiE-shDab1-EF1α-GFP or pSiE-shDsRed-EF1α-GFP using Lipofectamine 2000 (Invitrogen), incubated for 6 h at 37°C, followed by Lipofectamine transfection with the pDab1-IRES-mCh-WPRE overexpression construct. In the second experiment, cells were simultaneously transfected with pDab1-IRES-mCh-WPRE and either pSiE-shDab1-EF1α-GFP or pSiE-shDsRed-EF1α-GFP. Cells were subsequently cultured at 37°C for 48 h; briefly fixed in 4% paraformaldehyde (PFA) at room temperature for 20 min; blocked in PBS with 10% normal goat serum, 1% BSA, and 0.05% Triton X-100 for 1 h at room temperature; and incubated overnight at 4°C with primary antibody to rabbit (Rb) anti-Dab1 (1:2000; Pramatarova et al., 2008) and mouse anti-GFP (1:400, Invitrogen). Cells were washed twice in PBS, incubated with anti-rabbit IgG secondary antibody conjugated to Alexa Fluor 350 (Invitrogen) for 90 min at room temperature, washed, and imaged with a confocal microscope (Zeiss LSM 510).

Western blotting

For Western blotting, 293T cells were cultured in DMEM at 1.5×10^6 cells per 60 mm dish for 20 h at 37°C. Cells were transfected as previously described (Gong et al., 2007), protein was extracted using lysis buffer and RIPA, and protein concentration was determined using a spectrophotometer. Protein (50 μg) was resolved on a 10% SDS-PAGE gel (1.5 M Tris, pH 8.8, 30% acrylamide/bis-acrylamide, 10% SDS, 10% ammonium persulfate, and N,N,N′,N′-tetramethyl-ethylenediamine) using an electrophoresis apparatus (Bio-Rad). Proteins in the gel were transferred to a 0.45 μm nitrocellulose membrane using a Trans-Blot semidry blotter (Bio-Rad). The membrane was then blocked in a solution of 5% nonfat dry milk in Tris-buffered saline–Tween 20 (TBST) for 30 min at room temperature with slow agitation. It was then probed with primary goat anti-Dab1 antibody (1:500, Santa Cruz Biotechnology) in blocking buffer overnight at 4°C with agitation, washed in TBST, and incubated in secondary antibody conjugated with horseradish peroxidase (HRP) at 1:2000 in blocking buffer for 1 h. The membrane was washed, and ECL reagent (GE Healthcare) was applied as an HRP substrate. Immunoreactivity was detected and analyzed using the Gel-Doc XR System (Bio-Rad). The same membrane was washed and reprobed with anti-actin monoclonal antibody (1:2000; Santa Cruz Biotechnology) as an internal control to normalize Dab1 signal intensity.

Production and intrahippocampal injection of high-titer RV

Experiment 1. In this experiment, we used two RV stocks that varied in the genes encoded: CAG-GFP encoding for GFP, and CAG-GFP-IRES-CRE encoding for GFP and Cre-recombinase (Zhao et al., 2006). The plasmids used for the production of GFP-expressing RVs were a generous gift from Fred H. Gage (Salk Institute, La Jolla, CA).

RVs were produced by transient transfection of the 293T cell line as described previously (Zhao et al., 2006). RV stocks were concentrated by ultracentrifugation to working titers of $1 \times 10^7 - 2 \times 10^8$ pfu/ml. Adult male mice (7–8 weeks old) were anesthetized and placed in a stereotaxic frame. The scalp was incised, and holes were drilled in the skull. Targets with coordinates (in mm) relative to bregma in the anteroposterior, mediolateral, and dorsoventral planes were as follows: DG [−2.0, 1.4, 2.2]. In experimental animals, 1.5 μl per DG of virus solution was infused at 0.2 μl/min via glass micropipette, leaving the micropipettes in place an additional 5 min to ensure diffusion.

Experiment 2. The GP2–293 packaging cell line (Clontech) was transfected with an RV backbone (RV-pU6-shDab1-EF1α-GFP or RVpU6- dsRed-EF1α-GFP) and vesicular stomatitis virus glycoprotein G envelope protein to generate high-titer (10^7-10^9 cfu/ml) replication-incompetent RV vectors as previously described (Kron et al., 2010). For intrahippocampal injections, 8-week-old rats were anesthetized with a ketamine/xylazine mixture and placed on a water-circulating heating blanket. After positioning in a Kopf stereotaxic frame, a midline scalp incision was made, the scalp was reflected by hemostats to expose the skull, and bilateral burr holes were drilled. Either shDab1 (RV-pU6-shDab1-EF1α-GFP)

or control (RV-pU6-shDsRed-EF1α-GFP) RV was injected (2.5 μl of viral stock solution/site) into the left and right dentate gyrus over 20 min using a 5 μl Hamilton syringe, and the micropipette was left in place for an additional 2 min. Coordinates for injections (in mm from bregma and mm depth below the skull) were as follows: caudal 3.5, lateral 2.1, depth 3.8.

Tamoxifen administration

To conditionally delete *dab1* in postnatal DGC progenitors, mice received daily intraperitoneal injections of tamoxifen (TMX; dissolved in 10% EtOH/90% sunflower oil) at 180 mg/kg/d for 5 d on P28–P32 or 100 mg/kg/d on P7–P8. Animals in both groups survived until P60 (i.e., 52 d post-TMX for the P7–P8 group and 28 d for the P28–P32 group).

Tissue processing, histology, and immunohistochemistry

Animals were perfused with 4% PFA. The brains were then removed and postfixed, cryoprotected in 30% sucrose, and frozen. For some animals, a 0.37% sulfide fixative was also used for subsequent Timm staining (Kron et al., 2010). Coronal sections (50 μm thick in Experiment 1 and 40 μm thick in Experiment 2) were cut with a cryostat and fluorescence (single- and double-label) immunohistochemistry was performed on free-floating sections, as described previously (Parent et al., 1997, 1999; Kron et al., 2010), using the following antibodies: Rb anti-Prox1 (1:10,000, a gift from S. Pleasure, University of California at San Francisco, San Francisco, CA), Rb or Ms anti-GFP (1:1000 or 1:400, respectively, Invitrogen), Rb anti-Dab1 (Howell et al., 1997), goat anti-doublecortin (DCX, 1:500, Santa Cruz Biotechnology), Ms IgM anti-PSA-NCAM (1:500; 2–2b clone, Millipore Bioscience Research Reagents), Rb anti-T-brain2 (Tbr2; 1:500, Abcam), Ms anti-GFAP (1:250, Sigma), Rb anti-NG2 (1:500, Millipore Bioscience Research Reagents), Rb anti-S100α (1:400, Swant), or Ms anti-NF-M (1:500, Millipore Bioscience Research Reagents). For immunofluorescence, Alexa Fluor 488- or 594-conjugated goat anti-Ms or Rb IgG, or anti-Ms IgM secondary antibodies (1:400, Invitrogen) were used. In some cases, Tyramide-Plus signal amplification (1:50, catalog #SAT705A, PerkinElmer Life Sciences) was performed to ensure that all dendritic processes were brightly labeled for accurate quantification. Some tissue was also incubated in bisbenzamide (1:10,000, Sigma-Aldrich) to counterstain nuclei, and slides were coverslipped with anti-fade (Invitrogen). For electron microscopy, tissue slices were immunostained for GFP as above, postfixed in osmium tetroxide, and embedded in Araldite (Teijido et al., 2007).

For β-galactosidase staining, mice were perfused with 2% PFA and postfixed for 1 h in the same solution. After cryoprotection, 50 μm sections were cut using a cryostat. Sections were incubated at 37°C over night in the following solution: 200 mM $K_3Fe(CN)_6$, 200 mM $K_4Fe(CN)_6{}^{\circ}3H_2O$, 1 M $MgCl_2$, and 40 mg/ml X-gal in PBS-T (Triton-X 0.5%); all chemicals were from Sigma-Aldrich. Sections were mounted onto Superfrost Plus Slides (Thermo Fisher Scientific), then counterstained with neutral red, dehydrated in graded ethanols and xylene, and coverslipped with permount (Sigma-Aldrich).

For BrdU/Fos double staining, two TMX-treated *NestinCreER^{T2}/Dab1$^{flox/flox}$* mice were injected for 5 d, twice daily, with 100 mg/kg BrdU (dissolved in PBS). Four weeks after BrdU treatment, seizures were induced with pentylenetetrazole (PTZ; Sigma). Mice were initially injected with 30 mg/kg PTZ, and after 15 min they were injected with an additional 10 mg/kg. This procedure was repeated until the animals experienced repetitive seizures, usually after a total dose of ~60 mg/kg. Ninety minutes after the onset of seizures, mice were perfused and their brains were processed for immunohistochemistry. For BrdU immunohistochemistry, the BrdU antigen was exposed by incubating the sections in 1N HCl at 45°C for 30 min. Immunohistochemistry was performed using primary antibodies against Fos (rabbit anti-Fos polyclonal antibody; 1:1000; Calbiochem) and BrdU (rat anti-BrdU monoclonal antibody; 1:500; Accurate Chemicals). As secondary antibodies, we used Alexa Fluor 488 goat anti-rat, and Alexa Fluor 568 goat anti-rabbit (1:500; Invitrogen). Sections were incubated in primary antibodies for 48 h at 4°C, washed, and then incubated with secondary antibodies for 2 h at room temperature. After washing, sections were mounted with Mowiol.

Epifluorescence and confocal microscopy

Experiment 1. Images were collected using a Leica SPE confocal microscope. z-Stack projections were obtained using ImageJ (NIH), and dendritic length was measured using the ImageJ plugin NeuronJ (Meijering et al., 2004). One in six serial sections, spanning the entire DG, from three to four animals was analyzed per group, in a total of 20–40 cells per condition.

Experiment 2. Images were captured using a Leica DSMIRB epifluorescence microscope attached to a SPOT-RT digital camera or a Zeiss LSM 510 confocal microscope and colored in Adobe Photoshop. For confocal z-stacks, maximum intensity z-projections were analyzed in ImageJ.

Quantification of dendritic length and morphological subtypes. GFP-positive DGCs in rats injected with RV-U6-shDsRed-EF1α-GFP ($n = 4$) or RV-shDab1-EF1α-GFP ($n = 5$) were analyzed for dendritic length and dendritic complexity after immunolabeling for GFP using tyramide signal amplification. For each animal, a minimum of four cells with well labeled and properly located cell bodies and dendrites that extended to the hippocampal sulcus were analyzed. Confocal z-stacks were reconstructed, and Imaris software (Bitplane Scientific Software) was used to reconstruct and flatten the images for further analysis using the NeuronJ plug-in (Meijering et al., 2004) for ImageJ. Various brain sections from the same animal groups described above ($n = 5$/group) were used for quantification of the percentages of GFP-labeled cells with neuronal or glial morphology in the DGC layer and hilus (see Fig. 6). Between 20 and 70 cells were counted per animal in sections spanning the DG for a total of 372 cells (DGs from six sections per animal spaced 480 μm apart were counted bilaterally). Animals with <20 GFP-labeled cells were excluded from analysis. All observations were made by an observer blinded to experimental conditions.

Statistics

Comparisons among counts in multiple treatment groups were performed using a one-way ANOVA with Tukey's *post hoc t* tests. All values are reported as the mean + SEM, with $p < 0.05$ considered statistically significant.

Results

Reelin overexpression accelerates dendritic growth of adult-generated neurons

To study the impact of Reelin levels on adult neurogenesis, we used mice overexpressing Reelin under the control of the CaMKII promoter (*Reelin-OE* mice). This model specifically overexpresses this extracellular protein in the forebrain (including the DG of the hippocampus) from late postnatal stages onward (Pujadas et al., 2010). In contrast to *reeler* mice, this mouse model displays normal cortical lamination, thus allowing the analysis of neurogenesis independently of aberrant cortical organization. To analyze the development of adult-generated neurons at single-cell resolution, we injected GFP-expressing RV constructs in the DG of adult *Reelin-OE* and wild-type (*WT*) littermates (RV-CAG-GFP). Mice were killed at several postinjection times (2, 4, and 8 weeks) and processed for GFP immunohistochemistry (Fig. 1*A*). No major abnormalities were found in the gross morphology of these cells, with neurons from both genotypes projecting one or two primary apical dendrites that extended from the cell body through the GCL and branched in the molecular layer (ML) (Fig. 1*B*,*C*).

Examination of single labeled cells indicated that adult-generated neurons in *Reelin-OE* mice show accelerated dendritic development. To substantiate this observation, we quantified the dendritic tree of GFP-traced neurons. By 2 weeks of age, adult-generated GCs in *Reelin-OE* mice showed a dramatic increase in both the total extension of the dendritic tree and in the branching index, when compared with *WT* littermates (Fig. 1*D*,*E*). In contrast, by 4 and 8 weeks of age, the adult-generated neurons of both groups had a similar dendritic tree extension and branching in-

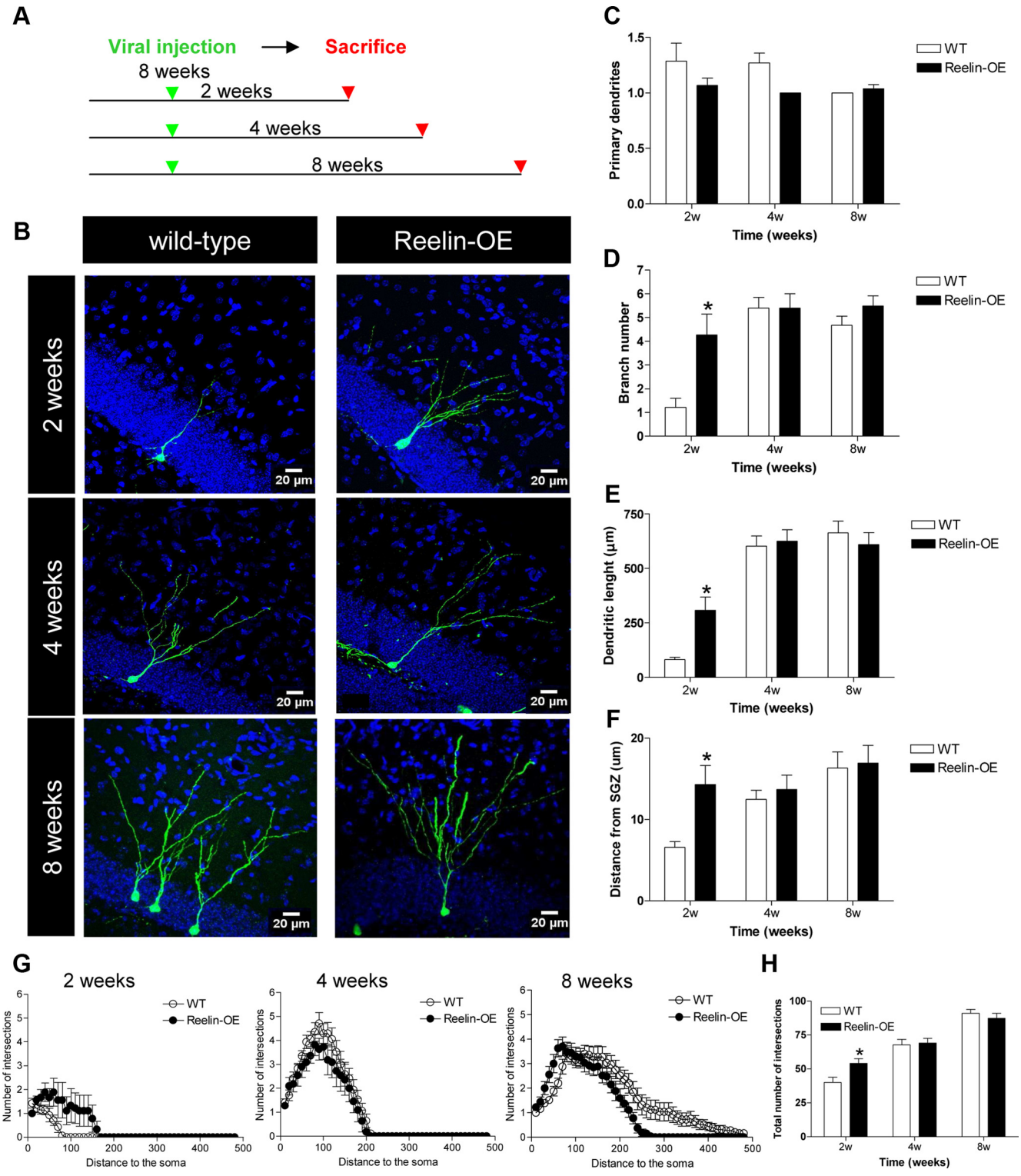

Figure 1. Reelin overexpression leads to faster development of the dendritic tree of adult-generated neurons. ***A***, Experimental design. Eight-week-old mice were injected with GFP-expressing retrovirus and killed at several time points after surgery. ***B***, Representative images of GFP-labeled adult-born neurons at 2, 4, and 8 weeks after injection in *WT* and *Reelin-OE* mice. ***C–E***, Quantification of morphological parameters of adult-generated neurons in *WT* and *Reelin-OE* mice at several time points after surgery. ***C***, The number of primary dendrites was similar between groups. ***D***, The number of branches in adult-generated neurons of *Reelin-OE* mice at 2 weeks after surgery was higher than in *WT* mice (*t* test: $p < 0.05$). ***E***, The dendritic length in adult-generated neurons of *Reelin-OE* mice at 2 weeks after surgery was higher than in *WT* mice (*t* test: $p < 0.05$). ***F***, Distance from the SGZ was greater in *Reelin-OE* mice at 2 weeks after injection (*t* test: $p < 0.05$). ***G***, ***H***, Sholl analysis shows fewer intersections in 2-week-old adult-generated neurons in *WT* than in *Reelin-OE* mice (*t* test: $p < 0.05$).

dex (Fig. 1*D*,*E*). This developmental difference was also evident using Sholl analysis, which showed a higher number of intersections in 2-week-old neurons from *Reelin-OE* mice when compared with *WT* littermates (Fig. 1*G*,*H*). However, this difference was no longer present at 4 and 8 weeks after injection. Moreover, 2-week-old labeled GC bodies of *Reelin-OE* mice tended to be located deeper (toward the ML aspect) in the GCL than in their *WT* counterparts. This difference was not detected at later time

points, suggesting faster migration (Fig. 1*F*), in agreement with a previous study (Pujadas et al., 2010).

These findings indicate that Reelin overexpression in the adult brain results in a dramatic and transient acceleration of dendritic development soon after adult neuron generation, with both groups of neurons reaching a similar dendritic complexity at 4–8 weeks.

Conditional loss of Reelin signaling impairs neurogenesis in the adult DG

reeler mutant mice display dramatic developmental alterations in the layering of the hippocampus (Stanfield and Cowan, 1979; Del Río et al., 1997; Drakew et al., 2002; Förster et al., 2002) and consequently are not adequate to study the effects of the absence of the Reelin signaling pathway specifically on adult neurogenesis. Dab1 is an adaptor protein that is essential for Reelin signaling, and its mutation leads to phenotypes identical to those of *reeler* mice (Howell et al., 1997; Sheldon et al., 1997). We thus decided to take advantage of previously generated conditional floxed-dab1 mice ($Dab1^{flox/flox}$) (Pramatarova et al., 2008). Although these mice have been reported to have lower Dab1 levels during development than WTs ($Dab1^{+/+}$) (Pramatarova et al., 2008), the adult brains of $Dab1^{flox/flox}$ and $Dab1^{+/+}$ mice showed similar levels of this protein, while Dab1 protein was absent in floxed mice crossed with a conditional ubiquitous Cre-recombinase line (*UbiCreER*^{T2} line; Fig. 2*A*). Furthermore, *NestinCreER*^{T2}/$Dab1^{flox/flox}$ mice did not present anatomical abnormalities in the DG (Fig. 2*C*; see also Fig. 4).

To visualize adult-generated cells in the DG of these animals, we generated *NestinCreER*^{T2}/*R26RYFP*/$Dab1^{flox/flox}$ triple-transgenic mice. Treatment of these mice with TMX leads to the removal of *dab1* and the expression of β-galactosidase and YFP (Fig. 2*B*). X-gal staining confirmed inactivation of *dab1* in putative dentate neuroprogenitor cells (Fig. 2*C*,*D*). We next examined the morphology of postnatal and young-adult neurons after TMX treatment at a range of postnatal ages (P7–P8 and P28–P32). After TMX treatment at P7–P8 followed by a 7 week survival period, YFP-immunoreactive DGCs in *NestinCreER*^{T2}/*R26RYFP*/$Dab1^{+/+}$ controls were well organized, normally oriented, and located mainly in the inner GCL (Fig. 2*E*). However, in *NestinCreER*^{T2}/*R26RYFP*/$Dab1^{flox/flox}$ mice, many YFP-positive neurons were found to be abnormally oriented in the GCL or located ectopically in the hilus, and occasionally in the ML (Fig. 2*F*, arrows). Furthermore, many labeled neurons appeared to display fewer dendrites in the ML and there were more labeled glia in the hilus (Fig. 2*F*, arrowhead). With later (P28–P32) TMX injections, followed by a 7 week survival period, the same abnormalities were present compared with controls (Fig. 2*G*,*H*). As expected, more labeled glia were seen when TMX was injected at younger ages. At both the P7–P8 and P28–P32 time points, however, conditional Dab1 deletion appeared to increase the amount of labeled glia compared with wild type (Fig. 2*E–H*).

To quantify defects in migration induced by postnatal loss of Dab1, we crossed WT *dab1* mice ($Dab1^{+/+}$), floxed *dab1* heterozygotes ($Dab1^{flox/+}$), and floxed *dab1* homozygotes ($Dab1^{flox/flox}$) with a *Nestin-Cre-ER*^{T2} line. DG morphology was examined by Prox1 immunohistochemistry after TMX treatment at either P7–P8 or P28–P32 and survival to P60, and the number of hilar ectopic DGCs was counted using unbiased stereology. The degree of GCL disorganization and increases in the numbers of hilar and ML ectopic DGCs were associated with a dose-dependent reduction of Dab1. Significant increases in hilar ectopic DGCs were detected in $Dab1^{flox/flox}$ mice receiving TMX treatment at P7–P8 or P28–P32, and in $Dab1^{flox/+}$ mice given TMX at P7–P8 compared with TMX-treated $Dab1^{+/+}$ littermate controls (Fig. 2*I*). $Dab1^{flox/flox}$ mice treated with TMX at P7–P8 had the most abnormal DG, with a more than sixfold increase in hilar ectopic DGCs (mean ± SEM, 13,010 ± 1233/mouse) compared with $Dab1^{+/+}$ controls (mean ± SEM, 1840 ± 376/mouse). As expected, the degree of abnormality was dependent in part upon the age at which mice received TMX treatment. Mice given TMX at younger ages showed more marked changes, consistent with larger numbers of Nestin-expressing progeny undergoing *dab1* deletion. To exclude a potential postnatal hypomorph effect on cell migration, we also compared the number of hilar ectopic Prox1+ cells in *NestinCreER*^{T2}/$Dab1^{flox/flox}$ mice in the presence or absence of P7–P8 TMX treatment. We found that TMX treatment led to a significant, more than fourfold increase in hilar ectopic DGCs [mean ± SEM, 1559 ± 261 with TMX ($n = 7$) vs 351 ± 65 without TMX ($n = 6$); $p = 0.005$, two-tailed t test].

To further examine the involvement of Dab1 in the migration of postnatal DGC progenitors, we immunostained brain sections for PSA-NCAM, a marker of neuroblasts in the DG. In *NestinCreER*^{T2}/$Dab1^{+/+}$ controls receiving TMX at P7–P8, these cells were properly located at the border of the DGC layer and hilus (Fig. 3*A*,*C*), whereas in *NestinCreER*^{T2}/$Dab1^{flox/flox}$ mice they were disorganized, showing abnormal placement in the hilus (Fig. 3*B*,*D*). These mice also displayed abnormal clusters or chains of presumptive migrating neuroblasts extending into the hilus from the subgranular zone (Fig. 3*D*, arrowheads). Migration in clusters or chains is typical of neuronophilic tangential, but not radial, migration. However, it is possible that the loss of Dab1 in radial glia alters the migration of DGC progenitors. The absence of Reelin signaling during development can interfere with radial glial scaffold formation in the DG, and others have proposed that this alteration underlies the abnormal DGC layer organization seen in mice with defective Reelin/Dab1 signaling (Förster et al., 2002; Weiss et al., 2003; Franco et al., 2011). Therefore, we used GFAP immunostaining to examine the effects of conditional Dab1 deletion on the radial glia scaffold. No obvious abnormalities in GFAP immunolabeling were present (Fig. 3*E*,*F*) despite abnormalities in the DGC layer (data not shown), thereby suggesting that the ectopic DGCs observed after postnatal loss of Dab1 are unlikely due to secondary influences on neuroblast migration caused by defects in the radial glial scaffold. In addition, *NestinCreER*^{T2}/$Dab1^{flox/flox}$ mice treated with TMX at P7–P8 displayed normal lamination of the hippocampus proper and cortex, as assessed by Nissl stain (data not shown).

These findings indicate that most neonatal or juvenile-born DGCs with inactivated Dab1 signaling migrate and integrate aberrantly into the adult DG. This observation thus supports the notion that Reelin signaling influences the migration and differentiation of DGC progenitors through Dab1.

Cell-autonomous inactivation of Dab1 in adult progenitors impairs dendritic development of adult-generated GCs

To analyze the influence of Reelin signaling on adult neurogenesis at the single-cell level, we inactivated Dab1 specifically in neuroprogenitor cells by injecting adult homozygous $Dab1^{flox/flox}$ mice with RV constructs expressing both Cre and GFP (RV-CAG-GFP-IRES-CRE); this approach allowed us to monitor the effect of cell-autonomous Dab1 inactivation in adult-generated neurons developing in a WT "milieu." Both $Dab1^{+/+}$ animals injected with RV-CAG-GFP-IRES-CRE and $Dab1^{flox/flox}$ mice injected with RV-CAG-GFP were used as controls. This RV backbone preferentially expresses in transit-amplifying progenitors rather

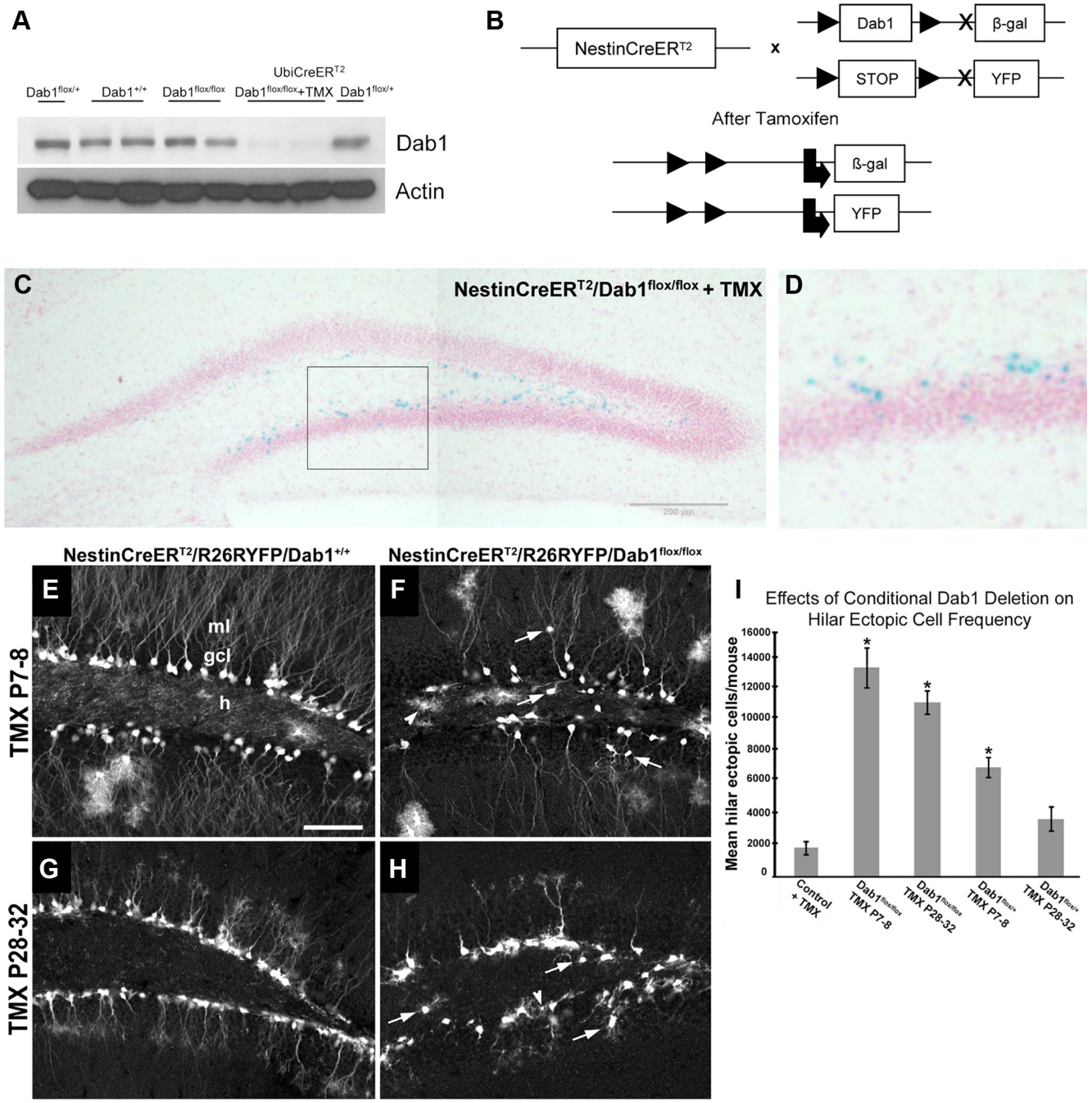

Figure 2. Characterization of the conditional Dab1 transgenic mouse. ***A***, Western blot of Dab1 expression in adult WT (*Dab1* $^{+/+}$), homozygous floxed Dab1 (*Dab1* $^{flox/flox}$), heterozygous floxed Dab1 (*Dab1* $^{flox/+}$), homozygous Dab1 crossed with a conditional ubiquitous Cre-line injected with tamoxifen (*UbiCreER* ^{T2}*/Dab1* $^{flox/flox}$ + TMX), and heterozygous Dab1 crossed with a conditional ubiquitous Cre-line (*UbiCreER* ^{T2}*/Dab1* $^{flox/+}$). ***B***, Scheme of the conditional Dab1 knockout triple-transgenic generation. Administration of TMX induces the removal of the *dab1* expression cassette by Cre-mediated recombination and consequent expression of the β-galactosidase reporter. At the same time, the drug induces the expression of YFP in Nestin-expressing cells. ***C***, ***D***, Expression of the β-galactosidase reporter in adult-generated neurons in the DG after tamoxifen injection in adult *NestinCreER* ^{T2}*/Dab1* $^{flox/flox}$ mice. ***E–H***, Expression of YFP in postnatally generated cells 7 weeks after injection of tamoxifen at P7–P8 or P28 –P32 in *NestinCreER* ^{T2}*/R26YFP/Dab1* $^{+/+}$ or *NestinCreER* ^{T2}*/R26YFP/Dab1* $^{flox/flox}$ mice. Arrows, Ectopically located cells; arrowhead, labeled glia in the hilus. ***I***, Quantification of hilar ectopic DGCs showed increases in *Nestin-CreER* ^{T2}*/Dab1* $^{flox/flox}$ mice treated with TMX at P7–P8 (*$p < 0.01$) or P28 –P32 (*$p < 0.001$), and in *Nestin-CreERT2/Dab1* $^{flox/+}$ given TMX at P7–P8 (*$p = 0.001$) versus TMX-treated *Nestin-CreERT2/Dab1* $^{+/+}$ controls (Con; early- and late-treated controls showed no difference and results were pooled). Scale bar: ***E–H*** (in ***E***), 75 μm.

than radial glia, as demonstrated by the finding that >90% of GFP-labeled cells coexpress Tbr2 or DCX at 2 d after RV-CAG-GFP injection (data not shown). Mice were killed at 2, 4, or 8 weeks after surgery. Immunostaining for Cre protein demonstrated that Cre was expressed in the nucleus of virtually all virus-infected neurons (data not shown). Examination of GFP-stained sections revealed that Dab1-deficient adult-generated neurons displayed severe abnormalities at all the stages studied (Fig. 4*A–F*). Interestingly, many Dab1-deficient neurons showed prominent basal dendrites extending to the hilus. A quantitative evaluation revealed that these neurons (from *Dab1* $^{flox/flox}$ mice injected with RV-CAG-GFP-IRES-CRE) had smaller dendritic trees and branched less profusely than WT neurons (from both *Dab1* $^{+/+}$ animals injected with RV-CAG-GFP-IRES-CRE and

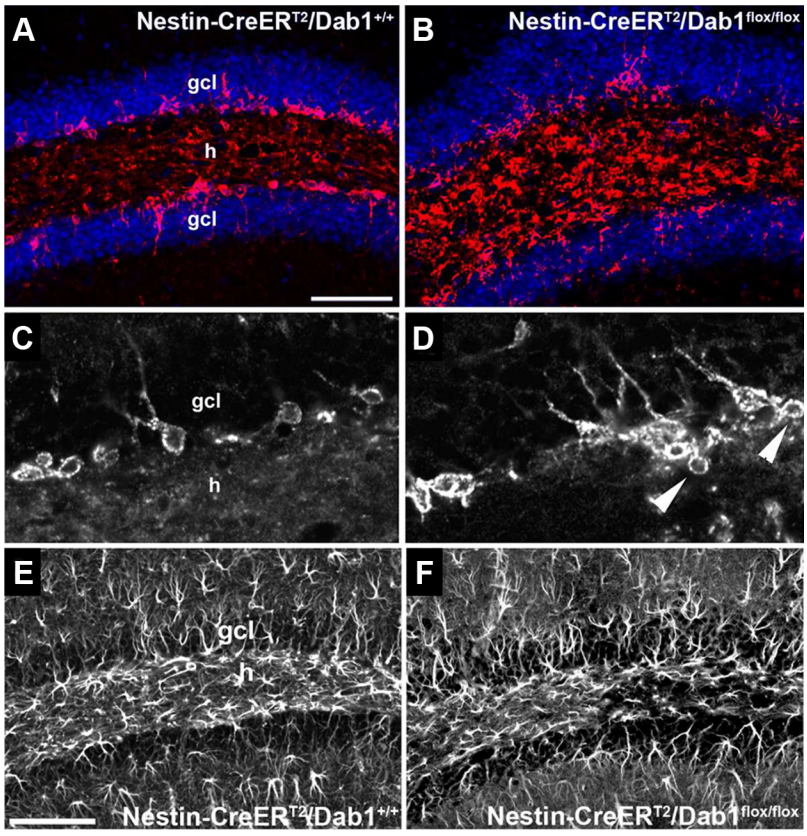

Figure 3. Conditional *dab1* deletion induces aberrant DGC migration. ***A***, ***C***, *NestinCreER^{T2}/Dab1$^{+/+}$* mice treated with TMX at P7–P8 had properly located neuroblasts in the dentate subgranular zone and inner granule cell layer (gcl) as assessed by PSA-NCAM immunoreactivity 52 d later. ***B***, ***D***, In *NestinCreER^{T2}/Dab1$^{flox/flox}$* mice treated with the same TMX regimen, PSA-NCAM immunolabeling was more disorganized, and many PSA-NCAM-positive cells appeared in the hilus (h). In addition, chains or clusters of presumptive migrating neuroblasts extended from the gcl into the h (***D***, arrowheads). Scale bar: (in ***A***), ***A***, ***B***, 50 μm; (in ***A***) ***C***, ***D***, 35 μm. ***E***, ***F***, GFAP immunostaining of DG from P60 *NestinCreER^{T2}/Dab1$^{+/+}$* control (***E***) and *NestinCreER^{T2}/Dab1$^{flox/flox}$* mice (***F***) treated with TMX at P7–P8. Labeled glia, including radial glia-like cells in the gcl, appeared unaffected by conditional loss of *dab1*. Scale bars: (in ***A***) ***A***, ***B***, 50 μm; ***C***, ***D***, 35 μm; (in ***E***) ***E***, ***F***, 150 μm.

Dab1$^{flox/flox}$ mice injected with RV-CAG-GFP). Interestingly, this held true both at early postinjection times (2–4 weeks) as well as at 8 weeks of age (Fig. 4*H*,*I*). Moreover, we found that Dab1-deficient DGCs transiently displayed significantly more primary dendrites than their *WT* counterparts, which typically had a single thick apical, primary dendrite (Fig. 4*G*). The differences in the dendritic tree were also evident in the Sholl analysis, with a higher number of intersections in control neurons when compared with Dab1-deficient ones (Fig. 4*J*,*K*).

Basal dendrites in DGCs have been associated with several neurological disorders including epilepsy and AD (Spigelman et al., 1998; Buckmaster and Dudek, 1999). We thus examined the presence and characteristics of basal dendrites in Dab1-deficient DGCs. A quantitative analysis revealed that up to 50–78% of Dab1-deficient neurons (depending on postinjection times) displayed basal dendrites, in marked contrast with control WT DGCs, in which these dendrites were not observed (Fig. 5*B*,*C*). Although the average basal dendritic extension per single cell was 165 ± 72 μm (Fig. 5*C*), many Dab1-deficient neurons showed dendritic trees extending and branching almost exclusively in the hilar region. Finally, quantitative analyses revealed that Dab1-deficient neurons not only displayed aberrant dendrites in the hilus, but also smaller dendritic trees in the ML, compared with control neurons (Fig. 5*D*). Together, the above data indicate that inactivation of the Reelin pathway in adult hippocampal progenitors leads to aberrant dendritic development of DGCs.

To confirm and further explore the effects of Dab1 knockdown in adult animals and in a different species, we used RV-mediated delivery of a Dab1 shRNA to suppress Dab1 expression in the DG of adult rats (Fig. 6). We generated an RV vector carrying a Dab1 shRNA sequence against the central fragment of Dab1 and an EF1α-driven GFP reporter (RV-shDab1-EF1α-GFP). An shRNA to DsRed (RV-shDsRed-EF1α-GFP), a gene not expressed in vertebrates, was used as a control. We first confirmed the capacity of shDab1-EF1α-GFP to knock down Dab1 expression by cotransfecting 293T cells with a Dab1-overexpressing vector carrying an mCherry reporter (Dab1-IRES-mCh) and either shDab1-EF1α-GFP or shDsRed-EF1α-GFP (Fig. 6*A–H*).

We next injected RV-shDab1-EF1α-GFP or RV-shDsRed-EF1α-GFP control vector into the DG of adult rats and examined the effects on GFP-labeled cells 4 weeks later (Fig. 6*I–M*). Similar to the conditional genetic deletion of Dab1 in mouse DGC progenitors and the retroviral Dab1 inactivation experiments, shRNA-mediated suppression of Dab1 in adult rat DGC progenitors decreased dendritic complexity, as 4-week-old DGCs showed more extensive dendritic arborization patterns after infection with control shRNA vector than those expressing RV-shDab1-EF1α-GFP (Fig. 6*I*,*J*). We quantified dendritic arborization of GFP-labeled cells and found that Dab1 shRNA decreased mean dendritic length by ~40% (Fig. 6*K*) and also reduced the mean numbers of secondary and tertiary dendritic branches by 48% and 72%, respectively (Fig. 6*L*,*M*).

Together, the above experiments using complementary approaches indicate that inactivation of the Reelin signaling cascade in adult hippocampal progenitor cells leads to aberrant dendritic development of DGCs in both mice and rats.

Loss of Dab1 leads to altered neuronal/glial fate

In addition to decreased dendritic arborization, Dab1 suppression produced an increase in labeled glia in adult rat DGC progenitors. Injection of control vector led to GFP labeling almost exclusively in neurons (Fig. 6*N*), but animals receiving RV-shDab1-EF1α-GFP injections showed frequent GFP labeling of cells with glial morphology (Fig. 6*O*). Strikingly, many sections from rats injected with Dab1 shRNA had almost exclusively labeled glia, including in the hilus and GCL (Fig. 6*P*). Subsets of these GFP-labeled cells coexpressed several glial markers, mainly S100β and GFAP, with a minority coexpressing NG2 (Fig. 6*R–T*). Quantification of the percentage of GFP-labeled cells that had a glial morphology revealed that animals injected with Dab1 shRNA had significantly more glia than those injected with dsRedshRNA (28.93 ± 9.8% glia in Dab1 shRNA-injected animals vs 3.82 ± 2.9% glia in DsRed shRNA-injected animals, $p <$

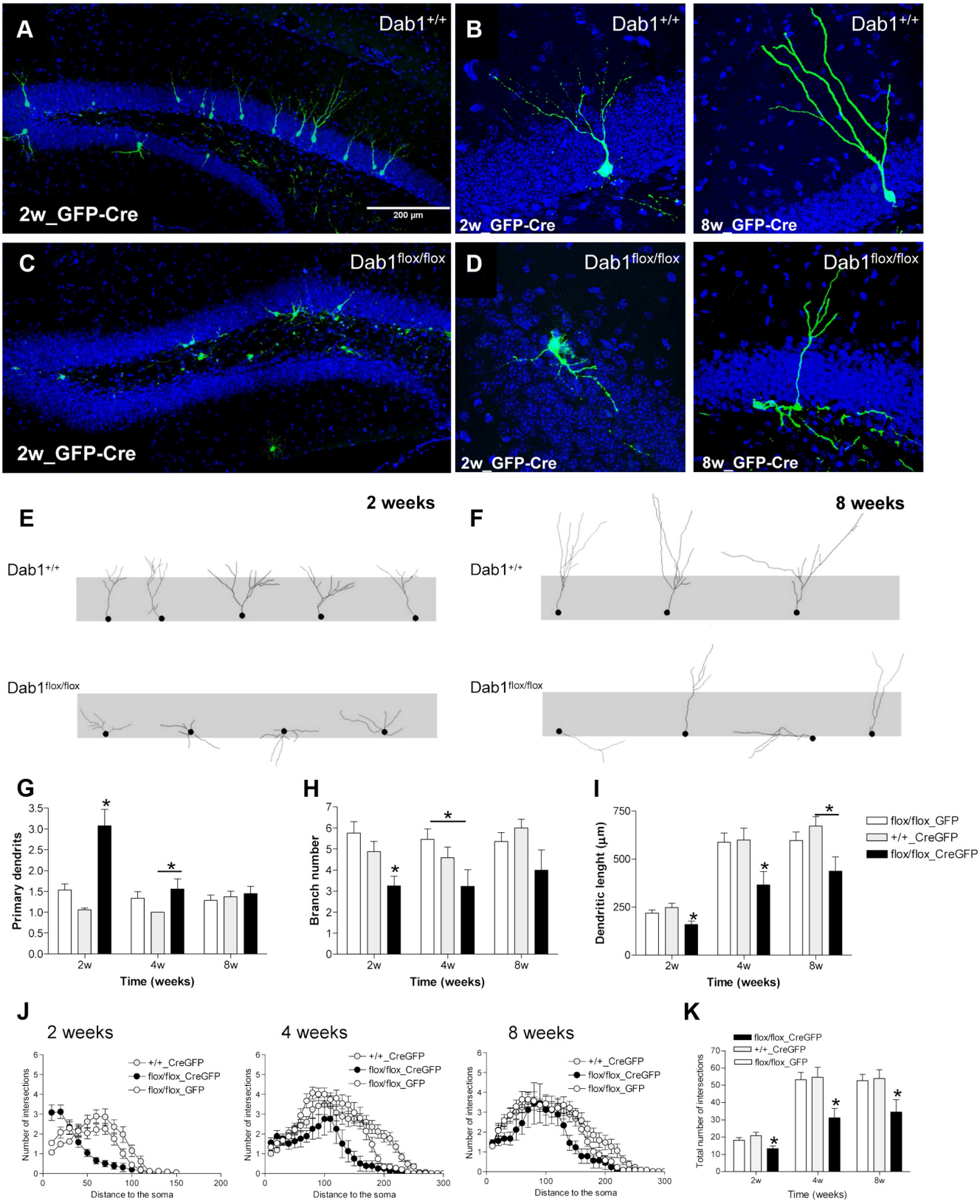

Figure 4. Dab1 deficiency leads to severe morphological alterations of adult-generated neurons. ***A–D***, Representative images of adult-generated neurons infected with GFP- and Cre-expressing retrovirus in Dab1 $^{+/+}$ and *Dab1* $^{flox/flox}$ mice 2 weeks after surgery. ***E***, ***F***, Tracings of adult-generated neurons at 2 and 8 weeks postsurgery in *Dab1* $^{+/+}$ and *Dab1* $^{flox/flox}$ mice. ***G–I***, Quantification of morphological parameters of adult-generated neurons infected with GFP only (GFP) or Cre and GFP (CreGFP) retroviruses in *Dab1* $^{+/+}$ and *Dab1* $^{flox/flox}$ mice. The number of primary dendrites in Dab1$^{flox/flox}$-GFP-Cre neurons was higher than in control groups at 2 weeks after surgery (ANOVA: $p < 0.05$; *post hoc*: $p < 0.05$) and in the WT-CreGFP group at 4 weeks (ANOVA: $p < 0.05$; *post hoc*: $p < 0.05$). The number of branches in Dab1$^{flox-flox}$-GFP-Cre neurons was greater than in control groups at 2 weeks after surgery (ANOVA: $p < 0.05$; *post hoc*: $p < 0.05$) and in the Dab1$^{flox/flox}$-GFP group at 4 weeks (ANOVA: $p < 0.05$; *post hoc*: $p < 0.05$). The dendritic length of Dab1$^{flox/flox}$-GFP-Cre neurons was higher than in control groups at 2 and 4 weeks after surgery (ANOVA: $p < 0.05$; *post hoc*: $p < 0.05$), and in the WT-CreGFP group at 8 weeks (ANOVA: $p < 0.05$; *post hoc*: $p < 0.05$). ***J***, ***K***, Sholl analysis. Dab1-deficient neurons have lower numbers of intersections than WT neurons at all the time points studied (ANOVA: $p < 0.05$; *post hoc*: $p < 0.05$).

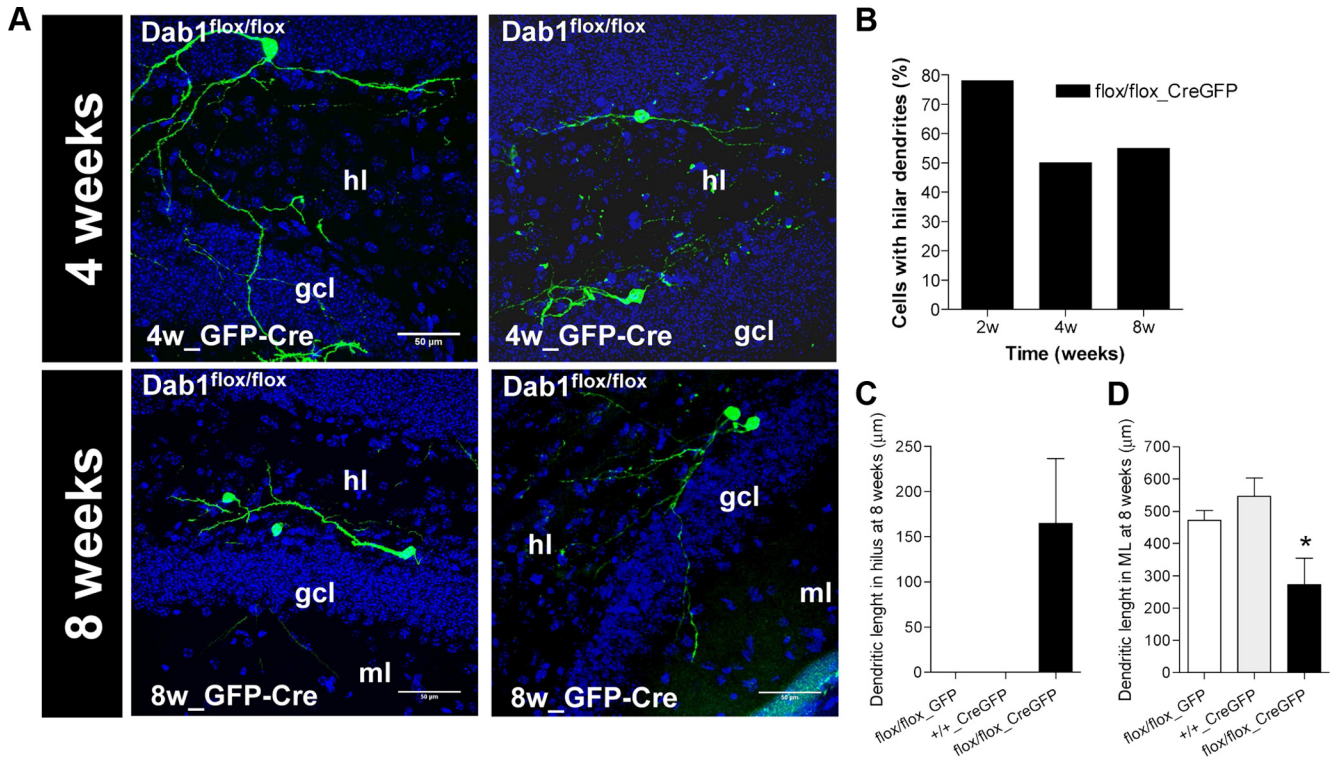

Figure 5. Dab1 knock-out adult-generated neurons exhibit ectopic basal dendrites in the hilus. ***A***, Representative images of Dab1 $^{flox/flox}$ neurons infected with GFP and Cre, with hilar dendrites at 4 and 8 weeks after surgery. hl, Hilus; gcl, granule cell layer; ml, molecular layer. ***B***, Between 50% and 78% of adult-generated cells in Dab1 $^{flox/flox}$ neurons infected with Cre exhibited hilar dendrites. This observation contrasts with the two control groups, in which no hilar dendrites were detected. ***C***, Presence of dendritic arborization in the hilus of Cre-infected Dab1 $^{flox/flox}$ neurons while this was absent in the other groups. ***D***, The dendritic arborization in the ML of Cre-infected Dab1 $^{flox/flox}$ neurons was lower than in control groups (ANOVA: $p < 0.05$; *post hoc*: $p < 0.05$).

0.05). Conversely, the number of GFP-positive cells with DGC morphology was decreased by Dab1 shRNA RV injection (67 ± 11% Dab1shRNA vs 85 ± 2% for controls), with a minority of cells (4–11%) of indeterminate morphology. These data indicate that the increase in glia occurs at the expense of granule neurons. In the Dab1 shRNA-injected animals showing labeled cells with glial morphology, 12.7% of these cells were located in the DGC layer while none were found in this layer in rats injected with DsRed shRNA. Many glia appeared in clusters near the subgranular zone. Interestingly, although not included in the analysis, rats injected with the Dab1 shRNA RV showed many glia located outside the GCL in the ML, and this was not observed in rats injected with the DsRed shRNA RV. These data suggest that suppression of the Reelin signaling pathway in adult progenitor cells modulates their differentiation into neuronal and glial cells.

Loss of Dab1 leads to aberrant synapse formation on DGC dendrites in the hilus

Persistent hilar basal dendrites on DGCs have been observed in rodent models of epilepsy (Spigelman et al., 1998; Buckmaster and Dudek, 1999; Ribak et al., 2000) and appear selectively in adult-generated DGCs (Jessberger et al., 2007; Walter et al., 2007; Kron et al., 2010). To study whether basal dendrites from adult-born Dab1-deficient DGCs receive synaptic contacts, we injected RV-CAG-GFP-IRES-CRE into the DGs of adult Dab1 $^{flox/flox}$ mice and performed electron microscopy studies of GFP-labeled neurons. Input synapses onto GFP-labeled adult-generated neurons were identified in 4-week-old DGCs and were very abundant at 8 weeks after injection (Fig. 7*A–G*). At both ages, presynaptic axon terminals contacting DGC dendrites displayed the fine structural features typical of mossy fiber collaterals in the hilus, including large accumulations of synaptic vesicles, occasional dense core vesicles, and asymmetric synaptic contacts. While some synaptic terminals were very large and corresponded to typical mossy fiber endings, others were considerably smaller and most likely corresponded to "en passant" mossy fiber boutons (Henze et al., 2000). Most GFP-labeled Dab1-deficient postsynaptic elements in the hilus were dendritic spines of variable shapes and sizes. These findings indicate that the lack of Reelin signaling in adult DGC progenitors not only results in abnormal dendritic growth and orientation but also in the establishment of aberrant innervation and circuitry, possibly involving mossy fiber collaterals in the hilus. In addition, deletion of Dab1 by P7–P8 TMX treatment of *NestinCreER* ^{T2}*/Dab1* $^{flox/flox}$ mice led to axon fasciculation defects of the suprapyramidal and infrapyramidal bundles, but did not cause mossy fiber sprouting in the dentate inner ML (data not shown).

To confirm that Dab1-deficient adult-generated neurons were effectively recruited into the DG circuitry, we injected BrdU into two *NestinCreER* ^{T2}*/Dab1* $^{flox/flox}$ mice that were previously treated with TMX. Four weeks after BrdU injection, we induced seizures using PTZ and perfused the animals 90 min later (Stone et al., 2011). We found that 90% of the BrdU-positive cells also expressed Fos, an activity-dependent immediate-early gene, thus indicating that 4-week-old Dab1-deficient adult-generated cells are already incorporated into DG circuits (Fig. 7*H*). Together with the above results, our data indicate that inactivation of the Reelin pathway in adult progenitors leads to the development of aberrant DGCs that, nevertheless, become synaptically and functionally integrated into adult circuits.

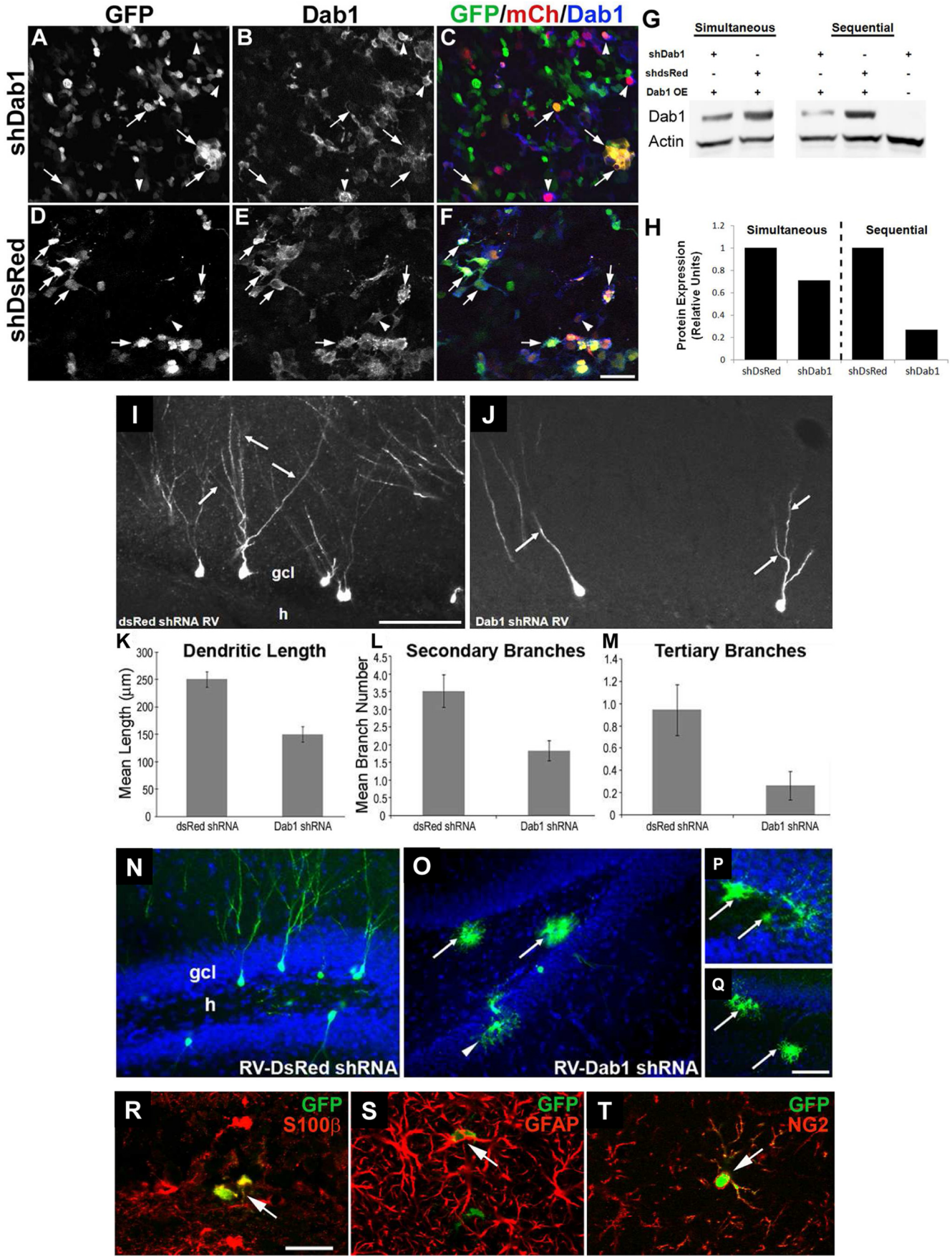

Figure 6. Less complex dendritic arbors form on adult-generated DGCs in rat after shRNA-induced Dab1 suppression. ***A–F***, Cultured 293T cells were cotransfected with Dab1 overexpression vector (pDab1-IRES-mCh-WPRE) and either pSiE-shDab1-EF1α-GFP (***A–C***) or pSiE-shDsRed-EF1α-GFP (***D–F***), and 48 h later were fixed and triple labeled for GFP, mCh, and Dab1. (*Figure legend continues.*)

Discussion

Our data from TMX-induced or Cre-recombinase-mediated deletion of *dab1* in mice, and RV-shRNA-mediated Dab1 suppression in rats indicate that Dab1 influences multiple stages of early postnatal and adult hippocampal neurogenesis. Aspects of DGC development and integration affected by loss of Dab1 include neuroprogenitor fate, dendritic maturation and orientation, and neuronal differentiation. Whereas Reelin overexpression accelerates dendritic maturation, a substantial fraction of Dab1-deficient cells in both the mouse and rat fail to develop appropriately complex dendritic processes. Furthermore, *dab1* knockout in adult-generated neurons results in ectopic synapse formation in the hilus. Nevertheless, these aberrant cells integrated into the circuit, as shown by immediate-early gene activation after induction of seizures. Our findings thus identify critical roles of the Reelin pathway in the maturation and integration of early postnatal and adult-generated DGCs. Although the contribution of several extracellular matrix proteins to the organization and migratory process in the SVZ/rostral migratory stream is well known (e.g., Tenascin) (Garcion et al., 2004), there are surprisingly few analyses of the contribution of the extracellular matrix to adult hippocampal neurogenesis and particularly to cell differentiation and dendritogenesis. One such study showed that the extracellular matrix protein laminin influences the makeup of postnatal hippocampal neural progenitor gap junctions and level of neurogenesis; however, this work was done entirely *in vitro* (Imbeault et al., 2009).

Previous studies indicate that the Reelin–Dab1 pathway is involved in regulating many events during embryonic development, including axonal targeting, dendritogenesis, laminar organization, and cell migration (for review, see Rice and Curran, 2001). Decreased dendritic complexity occurs in mice lacking Reelin both *in vivo* and *in vitro*, and this abnormality is rescued by addition of exogenous Reelin (Niu et al., 2004). Inhibitors of Dab1 activation also suppress dendrite outgrowth in embryonic hippocampal neurons (Niu et al., 2004), and early inactivation of a conditional *dab1* allele decreases dendritic complexity in the hippocampal CA1 region (Matsuki et al., 2008). Although Reelin expression persists in GABAergic interneurons in the adult cerebral cortex (Pesold et al., 1998; Haas et al., 2002; Abraham and Meyer, 2003; Gong et al., 2007) and Dab1 is expressed by DG neuroblasts and putative interneurons (Gong et al., 2007), the role of Reelin specifically in the adult brain is largely unknown. Thus, recent work indicates that Reelin overexpression in the adult brain results in increased synaptogenesis and hypertrophy of dendritic spines, further implicating the Reelin pathway in developmental processes that remain active in the adult brain (Pujadas et al., 2010). Moreover, Reelin positively regulates glutamatergic transmission and LTP in the adult brain (Herz and Chen, 2006; Teixeira et al., 2006; Pujadas et al., 2010).

Here we used transgenic and retroviral reporters along with Reelin gain-of-function and loss-of-function studies to address the involvement of the Reelin pathway in adult neurogenesis. We show that suppression of this pathway in adult progenitor cells shifts their fate toward glial cells. In adult *reeler* mice injected with BrdU to label dividing cells, the number of BrdU-labeled, GFAP-positive astrocytes is increased compared with *WT* mice, thereby indicating that adult neurogenesis is altered and that newly generated cells preferentially differentiate into astrocytes (Zhao et al., 2007). Furthermore, in neurospheres from the *dab1* mutant mouse *yotari*, and in the *yotari* brain *in vivo*, GFAP expression increases at the expense of neurons, further supporting the notion that Dab1 contributes to suppressing astroglial differentiation (Kwon et al., 2009). These results are consistent with our finding of increased labeled glia after RV-shRNA-mediated Dab1 knockdown. Some of the animals had many GFP-positive glial cells in the DGC layer, which were rarely observed in adult rat DGs infected with dsRedshRNA or RV reporters. Also, fewer labeled neurons were found in *NestinCreER^{T2}/R26YFP/Dab1$^{flox/flox}$* mice and in adult rats 4 weeks after Dab1 shRNA injection. These observations may reflect increased cell death after Dab1 knockdown, although an influence on cell proliferation cannot be excluded (Massalini et al., 2009). Recent evidence suggests that Reelin prevents retinoic acid-induced apoptotic cell death (Ohkubo et al., 2007), thereby implicating the Reelin–Dab1 pathway in cell survival.

Reeler and Dab1 mutant mice display overtly abnormal lamination in the cortex and DG (D'Arcangelo et al., 1995; Sheldon et al., 1997). In the postnatal brain, the Reelin–Dab1 pathway is thought to mediate tangential SVZ cell migration by directing chain-migrating progenitors to disperse from their chains (Hack et al., 2002). In mice lacking either Reelin receptors or Dab1, chain formation is severely compromised in the rostral migratory stream, and neuroblasts accumulate in the SVZ (Andrade et al., 2007). Conversely, Reelin overexpression results in altered migration in the olfactory bulb and premature exit of subventricular zone-derived migrating neurons from the rostral migratory stream (Pujadas et al., 2010; Courtès et al., 2011). The loss of Reelin in the epileptic DG may lead to aberrant chain migration of DGC precursors, thus implying that the Reelin–Dab1 pathway is necessary to maintain normal migration of adult-generated DGCs (Gong et al., 2007). In addition to aberrant chain migration, abnormal radial migration may arise secondary to a defective radial glial scaffold. In *reeler* mice, most radial glia-like cells in the DG are poorly differentiated and decreased in number and length (Förster et al., 2002), and *scrambler* and ApoER2/VLDLR-deficient mice also have alterations in the radial glial scaffold (Weiss et al., 2003). Although *dab1* is likely to be deleted in postnatal radial glia-like cells because they express Nestin, our data from *NestinCreER^{T2}/Dab1$^{flox/flox}$* animals do not show an overtly abnormal radial glial scaffold, as seen during defective Reelin signaling during embryonic development (Frotscher et al., 2003). Moreover, the RV construct that we used favors infection of

←

(*Figure legend continued.*) Yellow cells coexpressing mCh and GFP have lower Dab1 expression after knockdown with shDab1 (***A–C***, arrows) compared with similar cells in control cultures (***D–F***, arrows). Arrowheads in ***A–F*** denote cells with strong Dab1 expression in the setting of low or absent GFP. Note that mCh expression was lower in the shDsRed-expressing cultures (compare ***F*** with ***C***). Scale bar: (in ***F***) ***A–F***, 25 μm. ***G***, ***H***, Immunoblot (***G***) and densitometric quantification (***H***) of Dab1 protein expression in cultured 293T cells 48 h after transfection with varying combinations of Dab1 overexpression (OE) vector and shDab1 or shDsRed. Transfections were either performed simultaneously or with RNAi vector followed 6 h later by Dab1 OE vector (sequential). Sequential transfection of Dab1shRNA and then Dab1OE vector resulted in a >70% decrease in Dab1 protein levels compared with the control condition (***G***, lanes 4 and 5; ***H***, right-sided bars). ***I***, ***J***, RV-mediated expression of Dab1 shRNA in DGC progenitors markedly decreased dendritic arborization of GFP-labeled cells in the granule cell layer (gcl) of an adult rat (***J***, arrows) compared with control DsRed shRNA-infected DGCs (***I***, arrows). RV shRNA vectors were injected 4 weeks earlier. Scale bar: (in ***I***) ***I***, ***J***, 50 μm. ***K–M***, Quantification of dendritic complexity showed that Dab1 shRNA-expressing DGCs had decreased mean dendritic length (***K***, $p < 0.001$), and fewer secondary (***L***, $p < 0.005$) and tertiary branches (***M***, $p < 0.05$). ***N–Q***, Representative confocal images of adult rat DG 4 weeks after control RV-U6-shDsRed-EF1α-GFP injection (***N***) shows GFP-labeled DGCs with a normal appearance and no labeled glia. In contrast, after RV-U6-shDab1-EF1α-GFP injection, many labeled cells with glial morphology were evident in the DG (***O–Q***). Arrows indicate putative glial cells in the hilus (h), and the arrowhead in ***O*** denotes another in the gcl. Scale bar: (in ***Q***) ***O***, ***Q***, 50 μm; (in ***Q***) ***N***, ***P***, 25 μm. ***R–T***, Confocal images of sections through the DG of adult rats 4 weeks after injection of RV-U6-shDab1-EF1α-GFP double-immunolabeled for GFP (green) and S100β (***R***, red), GFAP (***S***, red), or NG2 (***T***, red). Arrows denote double-labeled cells in the dentate hilus. Scale bar: ***R***, 25 μm.

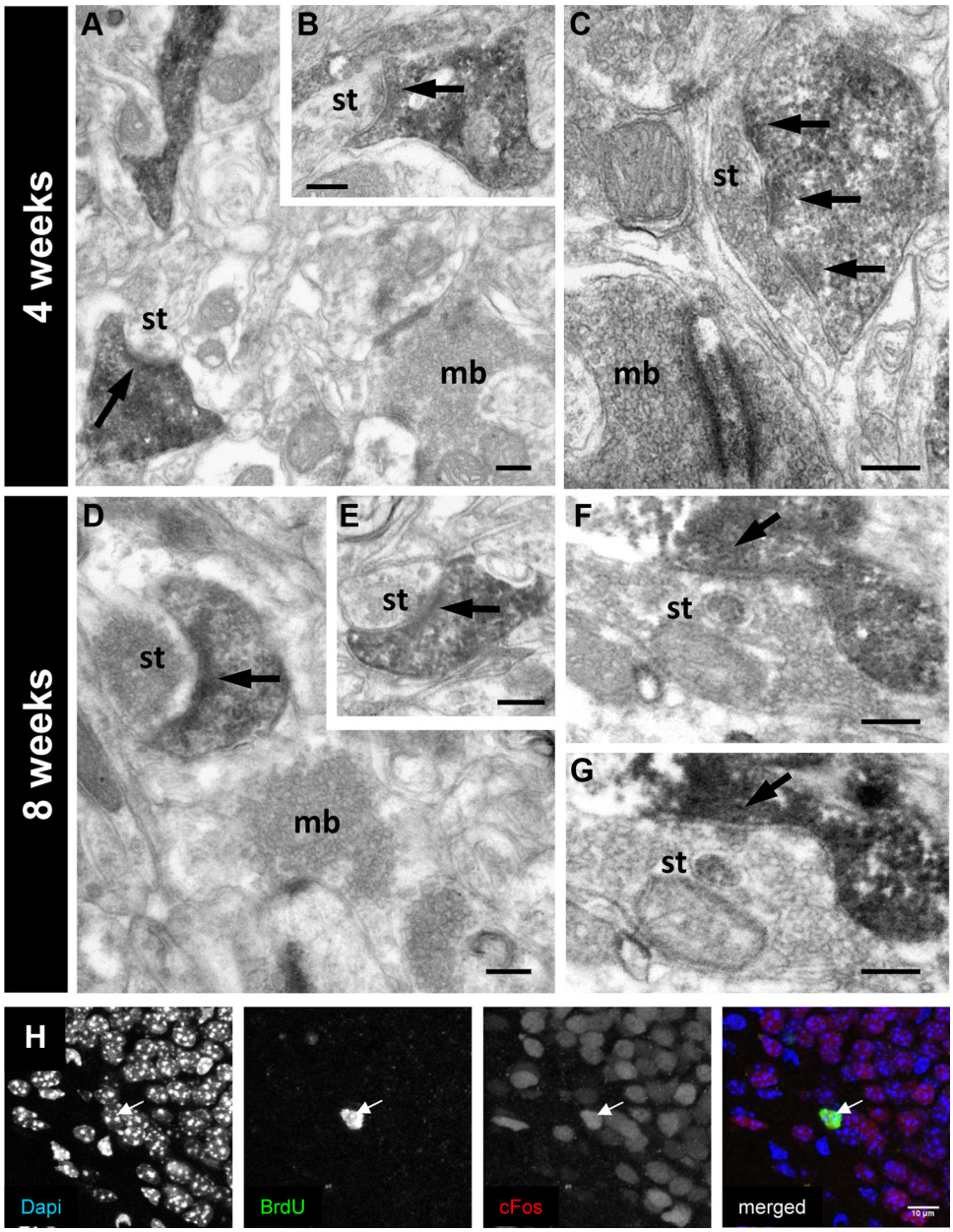

Figure 7. Basal dendrites from adult-generated Dab1-deficient neurons are integrated into the DG circuit. Electron microscopy of GFP-labeled basal dendrites, present in the hilus, from Dab1$^{flox/flox}$ neurons infected with CreGFP. ***A–C***, Labeled dendritic spines from basal dendrites at 4 weeks after injection receive synaptic contacts (arrows) from both immature axon terminals (***A***, ***B***) and boutons displaying a fully mature appearance (***C***); the synaptic contact (arrow) shown in ***A*** is illustrated in a serial section in ***B***. ***D–G***, At 8 weeks after injection, many GFP-labeled dendritic spines receive mature synaptic contacts (arrows) from unlabeled axon terminals. ***E*** and ***G*** are serial sections to those in ***D*** and ***F***, illustrating synaptic contacts. Some of the boutons contacting labeled spines displayed the typical features of the large mossy fiber boutons (mb), although most presynaptic axon terminals (st) were small, possibly corresponding to the small en passant boutons of mossy fiber collaterals or to commissural/associational axon terminals. ***H***, Seizure induction led to the expression of the activity-induced immediate early gene Fos (red staining in the merged image) in 4-week-old Dab1-deficient neurons (birth dated using BrdU, in green in the merged image). DAPI staining (left) is shown in blue in the merged image on the right. Scale bars: ***A–G***, 200 μm.

transit-amplifying progenitors over radial glia (Ge et al., 2006), as demonstrated by colocalization of the RV reporter with Tbr2 or DCX expression in the vast majority of labeled cells. This observation thus further supports the idea that Dab1 suppression in DGC progenitors directly influences the development of these cells rather than indirectly via altered radial glia. Our data are also consistent with previous work showing direct effects of Reelin on neonatal DG neuroblast migration *in vitro* (Gong et al., 2007).

The abnormalities caused by postnatal and adult loss of Dab1 in our study parallel those seen when Reelin/Dab1 signaling is disrupted during embryonic development. It is also important to note that inhibition of Notch1, which possibly interacts with Dab1, also leads to aberrant postnatal migration of GCs (Sibbe et al., 2009). Here we observed decreased dendritic complexity in cells infected with RV-CAG-GFP-IRES-CRE in *Dab1*$^{flox/flox}$ mice and with RV-shDab1-EF1α-GFP in the rat. The true effect is likely to be greater than that reported here, as our conservative analysis included only cells that extended dendrites all the way to the hippocampal sulcus; many more cells infected with RV-shDab1-EF1α-GFP had virtually no dendrites, but these were excluded to avoid cells with dendrites that left the plane of sectioning. Many of the YFP-positive cells in the TMX-treated *NestinCreER*^{T2}*/R26YFP/Dab1*$^{flox/flox}$ mice also had a more simplistic dendritic architecture. Conversely, Reelin overexpression

led to accelerated dendritic development of GCs. The previously described phenotypes thus strongly support the notion that the Reelin pathway and Dab1 contribute to proper dendritic maturation of both embryonic and adult-generated neurons.

An important finding of the present study is that DGC progenitors lacking Dab1 develop basal dendrites in the hilus, with many forming complex dendritic trees almost exclusively in the hilar region. This observation indicates that the Reelin pathway is required for proper dendritic orientation of adult-born GCs into the ML, thereby allowing correct synaptic integration with inputs from the entorhinal cortex and the commissural/associational pathways. Although Dab1-deficient adult-generated cells presented an abnormal morphology, they were integrated into DG circuits and formed ectopic synapses in the hilus with mossy fiber collaterals. These abnormal circuits might be relevant for understanding problems associated with several diseases in which Reelin levels are altered, such as temporal lobe epilepsy, autism, AD, depression, and schizophrenia (Fatemi et al., 2000; Torrey et al., 2005; Gong et al., 2007). In addition, these abnormal reverberant circuitries might interfere with the general function of the DG in pattern separation (Leutgeb et al., 2007; Aimone et al., 2011), possibly by impairing the sparse firing of DGCs. In fact, recent studies have proposed an essential role for adult neurogenesis in contextual discrimination (Clelland et al., 2009; Arruda-Carvalho et al., 2011; Sahay et al., 2011; Tronel et al., 2012).

Our study is the first to use an inducible model to conditionally delete *dab1* specifically in neural progenitors and to examine the involvement of Dab1 in early postnatal and adult DGC neurogenesis. With this model and shRNA-mediated knockdown, suppression of Dab1 is precisely timed and affects only a specific subset of cells. We found pleiotropic effects of Dab1 signaling on postnatal and adult DGC neurogenesis that involve dendritic outgrowth and differentiation, and integration into the DG circuit. Many of the developmental abnormalities induced by suppression of Dab1 in neonatal- and adult-generated neurons are similar to the aberrant plasticity that occurs in experimental, and possibly human, temporal lobe epilepsy, in which DG Reelin expression decreases after a precipitating injury (Gong et al., 2007). Further understanding of how Reelin–Dab1 signaling interacts with other pathways in DGC development may therefore offer new insight into strategies to correct brain disorders that involve abnormal neurogenesis.

References

Abraham H, Meyer G (2003) Reelin-expressing neurons in the postnatal and adult human hippocampal formation. Hippocampus 13:715–727.

Aimone JB, Deng W, Gage FH (2011) Resolving new memories: a critical look at the dentate gyrus, adult neurogenesis, and pattern separation. Neuron 70:589–596.

Alcántara S, Ruiz M, D'Arcangelo G, Ezan F, de Lecea L, Curran T, Sotelo C, Soriano E (1998) Regional and cellular patterns of reelin mRNA expression in the forebrain of the developing and adult mouse. J Neurosci 18:7779–7799.

Altman J, Das GD (1965) Post-natal origin of microneurones in the rat brain. Nature 207:953–956.

Andrade N, Komnenovic V, Blake SM, Jossin Y, Howell B, Goffinet A, Schneider WJ, Nimpf J (2007) ApoER2/VLDL receptor and Dab1 in the rostral migratory stream function in postnatal neuronal migration independently of Reelin. Proc Natl Acad Sci U S A 104:8508–8513.

Arruda-Carvalho M, Sakaguchi M, Akers KG, Josselyn SA, Frankland PW (2011) Posttraining ablation of adult-generated neurons degrades previously acquired memories. J Neurosci 31:15113–15127.

Buckmaster PS, Dudek FE (1999) In vivo intracellular analysis of granule cell axon reorganization in epileptic rats. J Neurophysiol 81:712–721.

Cameron HA, Woolley CS, McEwen BS, Gould E (1993) Differentiation of newly born neurons and glia in the dentate gyrus of the adult rat. Neuroscience 56:337–344.

Chen Y, Beffert U, Ertunc M, Tang TS, Kavalali ET, Bezprozvanny I, Herz J (2005) Reelin modulates NMDA receptor activity in cortical neurons. J Neurosci 25:8209–8216.

Clelland CD, Choi M, Romberg C, Clemenson GD Jr, Fragniere A, Tyers P, Jessberger S, Saksida LM, Barker RA, Gage FH, Bussey TJ (2009) A functional role for adult hippocampal neurogenesis in spatial pattern separation. Science 325:210–213.

Courtès S, Vernerey J, Pujadas L, Magalon K, Cremer H, Soriano E, Durbec P, Cayre M (2011) Reelin controls progenitor cell migration in the healthy and pathological adult mouse brain. PLoS One 6:e20430.

D'Arcangelo G, Miao GG, Chen SC, Soares HD, Morgan JI, Curran T (1995) A protein related to extracellular matrix proteins deleted in the mouse mutant reeler. Nature 374:719–723.

D'Arcangelo G, Homayouni R, Keshvara L, Rice DS, Sheldon M, Curran T (1999) Reelin is a ligand for lipoprotein receptors. Neuron 24:471–479.

Del Río JA, Heimrich B, Borrell V, Förster E, Drakew A, Alcántara S, Nakajima K, Miyata T, Ogawa M, Mikoshiba K, Derer P, Frotscher M, Soriano E (1997) A role for Cajal-Retzius cells and reelin in the development of hippocampal connections. Nature 385:70–74.

Drakew A, Deller T, Heimrich B, Gebhardt C, Del Turco D, Tielsch A, Förster E, Herz J, Frotscher M (2002) Dentate granule cells in reeler mutants and VLDLR and ApoER2 knockout mice. Exp Neurol 176:12–24.

Duan X, Chang JH, Ge S, Faulkner RL, Kim JY, Kitabatake Y, Liu XB, Yang CH, Jordan JD, Ma DK, Liu CY, Ganesan S, Cheng HJ, Ming GL, Lu B, Song H (2007) Disrupted-In-Schizophrenia 1 regulates integration of newly generated neurons in the adult brain. Cell 130:1146–1158.

Eisch AJ, Cameron HA, Encinas JM, Meltzer LA, Ming GL, Overstreet-Wadiche LS (2008) Adult neurogenesis, mental health, and mental illness: hope or hype? J Neurosci 28:11785–11791.

Fatemi SH, Earle JA, McMenomy T (2000) Reduction in Reelin immunoreactivity in hippocampus of subjects with schizophrenia, bipolar disorder and major depression. Mol Psychiatry 5:654–663, 571.

Faulkner RL, Jang MH, Liu XB, Duan X, Sailor KA, Kim JY, Ge S, Jones EG, Ming GL, Song H, Cheng HJ (2008) Development of hippocampal mossy fiber synaptic outputs by new neurons in the adult brain. Proc Natl Acad Sci U S A 105:14157–14162.

Förster E, Tielsch A, Saum B, Weiss KH, Johanssen C, Graus-Porta D, Müller U, Frotscher M (2002) Reelin, Disabled 1, and beta 1 integrins are required for the formation of the radial glial scaffold in the hippocampus. Proc Natl Acad Sci U S A 99:13178–13183.

Franco SJ, Martinez-Garay I, Gil-Sanz C, Harkins-Perry SR, Müller U (2011) Reelin regulates cadherin function via Dab1/Rap1 to control neuronal migration and lamination in the neocortex. Neuron 69:482–497.

Frotscher M, Haas CA, Förster E (2003) Reelin controls granule cell migration in the dentate gyrus by acting on the radial glial scaffold. Cereb Cortex 13:634–640.

Gao Z, Ure K, Ables JL, Lagace DC, Nave KA, Goebbels S, Eisch AJ, Hsieh J (2009) Neurod1 is essential for the survival and maturation of adult-born neurons. Nat Neurosci 12:1090–1092.

Garcion E, Halilagic A, Faissner A, ffrench-Constant C (2004) Generation of an environmental niche for neural stem cell development by the extracellular matrix molecule tenascin C. Development 131:3423–3432.

Ge S, Goh EL, Sailor KA, Kitabatake Y, Ming GL, Song H (2006) GABA regulates synaptic integration of newly generated neurons in the adult brain. Nature 439:589–593.

Ge S, Sailor KA, Ming GL, Song H (2008) Synaptic integration and plasticity of new neurons in the adult hippocampus. J Physiol 586:3759–3765.

Gong C, Wang TW, Huang HS, Parent JM (2007) Reelin regulates neuronal progenitor migration in intact and epileptic hippocampus. J Neurosci 27:1803–1811.

Groc L, Choquet D, Stephenson FA, Verrier D, Manzoni OJ, Chavis P (2007) NMDA receptor surface trafficking and synaptic subunit composition are developmentally regulated by the extracellular matrix protein Reelin. J Neurosci 27:10165–10175.

Haas CA, Frotscher M (2010) Reelin deficiency causes granule cell dispersion in epilepsy. Exp Brain Res 200:141–149.

Haas CA, Dudeck O, Kirsch M, Huszka C, Kann G, Pollak S, Zentner J, Frotscher M (2002) Role for reelin in the development of granule cell dispersion in temporal lobe epilepsy. J Neurosci 22:5797–5802.

Hack I, Bancila M, Loulier K, Carroll P, Cremer H (2002) Reelin is a detachment signal in tangential chain-migration during postnatal neurogenesis. Nat Neurosci 5:939–945.

Heinrich C, Nitta N, Flubacher A, Müller M, Fahrner A, Kirsch M, Freiman T, Suzuki F, Depaulis A, Frotscher M, Haas CA (2006) Reelin deficiency and displacement of mature neurons, but not neurogenesis, underlie the formation of granule cell dispersion in the epileptic hippocampus. J Neurosci 26:4701–4713.

Henze DA, Urban NN, Barrionuevo G (2000) The multifarious hippocampal mossy fiber pathway: a review. Neuroscience 98:407–427.

Herz J, Chen Y (2006) Reelin, lipoprotein receptors and synaptic plasticity. Nat Rev Neurosci 7:850–859.

Hiesberger T, Trommsdorff M, Howell BW, Goffinet A, Mumby MC, Cooper JA, Herz J (1999) Direct binding of Reelin to VLDL receptor and ApoE receptor 2 induces tyrosine phosphorylation of disabled-1 and modulates tau phosphorylation. Neuron 24:481–489.

Howell BW, Hawkes R, Soriano P, Cooper JA (1997) Neuronal position in the developing brain is regulated by mouse disabled-1. Nature 389:733–737.

Imbeault S, Gauvin LG, Toeg HD, Pettit A, Sorbara CD, Migahed L, DesRoches R, Menzies AS, Nishii K, Paul DL, Simon AM, Bennett SA (2009) The extracellular matrix controls gap junction protein expression and function in postnatal hippocampal neural progenitor cells. BMC Neurosci 10:13.

Jessberger S, Zhao C, Toni N, Clemenson GD Jr, Li Y, Gage FH (2007) Seizure-associated, aberrant neurogenesis in adult rats characterized with retrovirus-mediated cell labeling. J Neurosci 27:9400–9407.

Jessberger S, Aigner S, Clemenson GD Jr, Toni N, Lie DC, Karalay O, Overall R, Kempermann G, Gage FH (2008) Cdk5 regulates accurate maturation of newborn granule cells in the adult hippocampus. PLoS Biol 6:e272.

Karalay O, Doberauer K, Vadodaria KC, Knobloch M, Berti L, Miquelajauregui A, Schwark M, Jagasia R, Taketo MM, Tarabykin V, Lie DC, Jessberger S (2011) Prospero-related homeobox 1 gene (Prox1) is regulated by canonical Wnt signaling and has a stage-specific role in adult hippocampal neurogenesis. Proc Natl Acad Sci U S A 108:5807–5812.

Kim JY, Duan X, Liu CY, Jang MH, Guo JU, Pow-anpongkul N, Kang E, Song H, Ming GL (2009) DISC1 regulates new neuron development in the adult brain via modulation of AKT-mTOR signaling through KIAA1212. Neuron 63:761–773.

Kron MM, Zhang H, Parent JM (2010) The developmental stage of dentate granule cells dictates their contribution to seizure-induced plasticity. J Neurosci 30:2051–2059.

Kuhn HG, Dickinson-Anson H, Gage FH (1996) Neurogenesis in the dentate gyrus of the adult rat: age-related decrease of neuronal progenitor proliferation. J Neurosci 16:2027–2033.

Kwon IS, Cho SK, Kim MJ, Tsai MJ, Mitsuda N, Suh-Kim H, Lee YD (2009) Expression of Disabled 1 suppresses astroglial differentiation in neural stem cells. Mol Cell Neurosci 40:50–61.

Lagace DC, Whitman MC, Noonan MA, Ables JL, DeCarolis NA, Arguello AA, Donovan MH, Fischer SJ, Farnbauch LA, Beech RD, DiLeone RJ, Greer CA, Mandyam CD, Eisch AJ (2007) Dynamic contribution of nestin-expressing stem cells to adult neurogenesis. J Neurosci 27:12623–12629.

Lagace DC, Benavides DR, Kansy JW, Mapelli M, Greengard P, Bibb JA, Eisch AJ (2008) Cdk5 is essential for adult hippocampal neurogenesis. Proc Natl Acad Sci U S A 105:18567–18571.

Lemaire V, Tronel S, Montaron MF, Fabre A, Dugast E, Abrous DN (2012) Long-lasting plasticity of hippocampal adult-born neurons. J Neurosci 32:3101–3108.

Leutgeb JK, Leutgeb S, Moser MB, Moser EI (2007) Pattern separation in the dentate gyrus and CA3 of the hippocampus. Science 315:961–966.

Lie DC, Colamarino SA, Song HJ, Désir é L, Mira H, Consiglio A, Lein ES, Jessberger S, Lansford H, Dearie AR, Gage FH (2005) Wnt signalling regulates adult hippocampal neurogenesis. Nature 437:1370–1375.

Massalini S, Pellegatta S, Pisati F, Finocchiaro G, Farace MG, Ciafr è SA (2009) Reelin affects chain-migration and differentiation of neural precursor cells. Mol Cell Neurosci 42:341–349.

Matsuki T, Pramatarova A, Howell BW (2008) Reduction of Crk and CrkL expression blocks reelin-induced dendritogenesis. J Cell Sci 121:1869–1875.

Meijering E, Jacob M, Sarria JC, Steiner P, Hirling H, Unser M (2004) Design and validation of a tool for neurite tracing and analysis in fluorescence microscopy images. Cytometry A 58:167–176.

Niu S, Renfro A, Quattrocchi CC, Sheldon M, D'Arcangelo G (2004) Reelin promotes hippocampal dendrite development through the VLDLR/ApoER2-Dab1 pathway. Neuron 41:71–84.

Ohkubo N, Vitek MP, Morishima A, Suzuki Y, Miki T, Maeda N, Mitsuda N (2007) Reelin signals survival through Src-family kinases that inactivate BAD activity. J Neurochem 103:820–830.

Olson EC, Kim S, Walsh CA (2006) Impaired neuronal positioning and dendritogenesis in the neocortex after cell-autonomous Dab1 suppression. J Neurosci 26:1767–1775.

Parent JM, Yu TW, Leibowitz RT, Geschwind DH, Sloviter RS, Lowenstein DH (1997) Dentate granule cell neurogenesis is increased by seizures and contributes to aberrant network reorganization in the adult rat hippocampus. J Neurosci 17:3727–3738.

Parent JM, Tada E, Fike JR, Lowenstein DH (1999) Inhibition of dentate granule cell neurogenesis with brain irradiation does not prevent seizure-induced mossy fiber synaptic reorganization in the rat. J Neurosci 19:4508–4519.

Pesold C, Impagnatiello F, Pisu MG, Uzunov DP, Costa E, Guidotti A, Caruncho HJ (1998) Reelin is preferentially expressed in neurons synthesizing gamma-aminobutyric acid in cortex and hippocampus of adult rats. Proc Natl Acad Sci U S A 95:3221–3226.

Pramatarova A, Chen K, Howell BW (2008) A genetic interaction between the APP and Dab1 genes influences brain development. Mol Cell Neurosci 37:178–186.

Pujadas L, Gruart A, Bosch C, Delgado L, Teixeira CM, Rossi D, de Lecea L, Martínez A, Delgado-García JM, Soriano E (2010) Reelin regulates postnatal neurogenesis and enhances spine hypertrophy and long-term potentiation. J Neurosci 30:4636–4649.

Qiu S, Zhao LF, Korwek KM, Weeber EJ (2006) Differential reelin-induced enhancement of NMDA and AMPA receptor activity in the adult hippocampus. J Neurosci 26:12943–12955.

Ribak CE, Tran PH, Spigelman I, Okazaki MM, Nadler JV (2000) Status epilepticus-induced hilar basal dendrites on rodent granule cells contribute to recurrent excitatory circuitry. J Comp Neurol 428:240–253.

Rice DS, Curran T (2001) Role of the reelin signaling pathway in central nervous system development. Annu Rev Neurosci 24:1005–1039.

Rice DS, Sheldon M, D'Arcangelo G, Nakajima K, Goldowitz D, Curran T (1998) Disabled-1 acts downstream of Reelin in a signaling pathway that controls laminar organization in the mammalian brain. Development 125:3719–3729.

Sahay A, Scobie KN, Hill AS, O'Carroll CM, Kheirbek MA, Burghardt NS, Fenton AA, Dranovsky A, Hen R (2011) Increasing adult hippocampal neurogenesis is sufficient to improve pattern separation. Nature 472:466–470.

Sheldon M, Rice DS, D'Arcangelo G, Yoneshima H, Nakajima K, Mikoshiba K, Howell BW, Cooper JA, Goldowitz D, Curran T (1997) Scrambler and yotari disrupt the disabled gene and produce a reeler-like phenotype in mice. Nature 389:730–733.

Sibbe M, Förster E, Basak O, Taylor V, Frotscher M (2009) Reelin and Notch1 cooperate in the development of the dentate gyrus. J Neurosci 29:8578–8585.

Spigelman I, Yan XX, Obenaus A, Lee EY, Wasterlain CG, Ribak CE (1998) Dentate granule cells form novel basal dendrites in a rat model of temporal lobe epilepsy. Neuroscience 86:109–120.

Stanfield BB, Cowan WM (1979) The morphology of the hippocampus and dentate gyrus in normal and reeler mice. J Comp Neurol 185:393–422.

Stone SS, Teixeira CM, Zaslavsky K, Wheeler AL, Martinez-Canabal A, Wang AH, Sakaguchi M, Lozano AM, Frankland PW (2011) Functional convergence of developmentally and adult-generated granule cells in dentate gyrus circuits supporting hippocampus-dependent memory. Hippocampus 21:1348–1362.

Sun B, Halabisky B, Zhou Y, Palop JJ, Yu G, Mucke L, Gan L (2009) Imbalance between GABAergic and glutamatergic transmission impairs adult neurogenesis in an animal model of Alzheimer's disease. Cell Stem Cell 5:624–633.

Teijido O, Casaroli-Marano R, Kharkovets T, Aguado F, Zorzano A, Palacín M, Soriano E, Martínez A, Estévez R (2007) Expression patterns of MLC1 protein in the central and peripheral nervous systems. Neurobiol Dis 26:532–545.

Teixeira CM, Pomedli SR, Maei HR, Kee N, Frankland PW (2006) Involvement of the anterior cingulate cortex in the expression of remote spatial memory. J Neurosci 26:7555–7564.

Tissir F, Goffinet AM (2003) Reelin and brain development. Nat Rev Neurosci 4:496–505.

Toni N, Laplagne DA, Zhao C, Lombardi G, Ribak CE, Gage FH, Schinder AF (2008) Neurons born in the adult dentate gyrus form functional synapses with target cells. Nat Neurosci 11:901–907.

Torrey EF, Barci BM, Webster MJ, Bartko JJ, Meador-Woodruff JH, Knable MB (2005) Neurochemical markers for schizophrenia, bipolar disorder, and major depression in postmortem brains. Biol Psychiatry 57:252–260.

Tronel S, Belnoue L, Grosjean N, Revest JM, Piazza PV, Koehl M, Abrous DN (2012) Adult-born neurons are necessary for extended contextual discrimination. Hippocampus 22:292–298.

van Praag H, Schinder AF, Christie BR, Toni N, Palmer TD, Gage FH (2002) Functional neurogenesis in the adult hippocampus. Nature 415:1030–1034.

Walter C, Murphy BL, Pun RY, Spieles-Engemann AL, Dancer SC (2007) Pilocarpine-induced seizures cause selective time-dependent changes to adult-generated hippocampal dentate granule cells. J Neurosci 27:7541–7552.

Weiss KH, Johanssen C, Tielsch A, Herz J, Deller T, Frotscher M, Förster E (2003) Malformation of the radial glial scaffold in the dentate gyrus of reeler mice, scrambler mice, and ApoER2/VLDLR-deficient mice. J Comp Neurol 460:56–65.

Zhao C, Teng EM, Summers RG Jr, Ming GL, Gage FH (2006) Distinct morphological stages of dentate granule neuron maturation in the adult mouse hippocampus. J Neurosci 26:3–11.

Zhao S, Chai X, Frotscher M (2007) Balance between neurogenesis and gliogenesis in the adult hippocampus: role for reelin. Dev Neurosci 29:84–90.